RSC Advances

ROYAL SOCIETY OF CHEMISTRY

www.rsc.org/advances

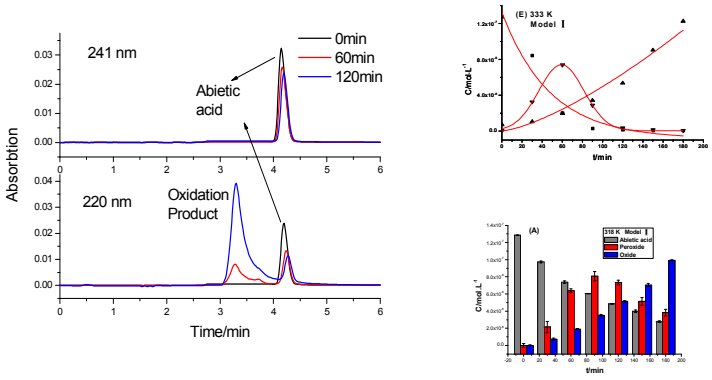

A kinetic study on the oxidation of abietic acid, providing new basic data.

Thermal Oxidation Reaction Process and Oxidation Kinetics of Abietic Acid

Fan Ren, Yan-Fei Zheng, Xiong-Min Liu*, Qiong-Qiong Yang, Qiang Zhang and Fang Shen

School of Chemistry and Chemical Engineering, Guangxi University, Nanning 530004 , Guangxi , China

*Corresponding author:

Prof. Dr. Xiong-Min Liu

School of Chemistry and Chemical Engineering, Guangxi University, Nanning 530004, Guangxi, China

Phone: +86 138 7713 6730

e-mail : xmliu1@gxu.edu.cn (Xiong-Min Liu)

Abstract

Thermal oxidation reaction process and oxidation kinetics of abietic acid was investigated by using a self designed gas-solid reaction equipment. Oxidation product and intermediates of oxidation reaction of abietic acid were tracked by LC-MS. The results revealed a two-step oxidation reaction of abietic acid: Abietic acid formed the peroxide first, followed by cracking which formed hydroxyl contained oxidized abietic acid. Both of them followed pseudo-first order reaction, in which the kinetic equation of the first step is $r_1=c_A\times3.51\times10^3\times\exp(-58.96\times10^3/RT)$, active energy is 58.96 kJ/mol. The kinetic equation of the second step is $r_2=c_O\times6.09\times10^5\times\exp(-48.06\times10^3/RT)$, active energy is 48.06 kJ/mol. The kinetic equation of the total reaction is $r_a=c_a\times1.12\times10^6\times\exp(49.51\times10^3/RT)$, apparent active energy is 49.51 kJ/mol.

Introduction

Rosin is a renewable resource obtained by the distillation of the exudates of pines trees. It is composed mostly of abietic acid and other rosin acids which plays an important role in the application of everyday life, e.g., in painting[1], adhesive[2] and biochemical synthesis[3]. China has the world's biggest pine forest cover, it is necessary for us to take full advantage of the resource and create economic benefit. However, due to the active structure of conjugated double bonds, resin acids and its products, such as colophony are instable against air, heat, and light, as well as their sensitivity to mineral acids. These oxidation behavior lead to the color fastness and limit the application of rosin immediately, which are the main reason for its reduced cost similarly. In order to improve the antioxidant abilities and wetherability of rosin products, a series of studies have focused on the oxidation mechanism, oxidation products and oxidation kinetics.

In aspect of oxidation products and oxidation process, Harris[4] assumed that auto-oxidation of abietic acid has two paths. One starts from addition of O_2 and C13 C14 double bond. As formed peroxide will cleavage into two hydroxyl. The second is a substitute reaction between active methylene C12 and O_2, which forms peroxide. After cleavage, stable hydroxyl is formed. Enoki[5] studied several oxidation products of resin acids in α-pinene solution. Prinz[6] identified 6 known oxidation products of abietic acid and methyl ester in different storage conditions. He also pointed out that sensitive positions of the reaction are C7 and C13.

Several investigations have studied the kinetics of resin acids, but there are few reports on kinetics of thermal oxidation reaction. Ritchie[7] reported the isomerization kinetic of L-pimaric acid and neoabietic acid under absolute ethyl alcohol catalyzed by strong acid.

Lawrence[8] studied kinetic of thermal catalyzed isomerization of abietic acid, L-pimaric acid, neoabietic acid and palustric acid at 150-200 °C. Pastorova[9] proposed that isomerization of abietic acid type resin acid forms stable dehydroabietic acid. In addition, they discussed four oxidation paths. Ladero[10, 11] investigated the kinetic of the esterification of rosin and polyols. Rongxiu Qin[12, 13] performed kinetic study on room temperature oxidation of abietic acid, colophony and rosin and pointed out that oxidation of abietic acid was peso-first order reaction with an active energy of 50.29 kJ/mol. Jialing Liu[14] explored kinetic study on UV-induced oxidation of colophony and obtained kinetic data under 365 nm irradiation. When applying UV spectroscopy to kinetic study, iteration is required to eliminate the influence of product. The main problem is that an UV absorptive intermediate will disturb iteration. It must be mentioned that oxidation of abietic acid contains multiple steps which is not able to be identified by UV spectroscopy, and the researchers investigated the global kinetic of oxidation reaction is a preliminary state. Therefore, it is necessary to obtain more precise and detailed data for the reaction kinetics in order to seek a more suitable method for anti-oxidation.

The aim of this work is to continue the investigations regarding the thermal oxidation reaction process and oxidation kinetics of abietic acid. More precisely, the article presents a novel micro solid-state reactor to conduct the oxidation reaction of abeitic acid, using the polyethylene film fixed by two aluminum sheets. In this way, abietic acid formed as a membrane on the PE film, making the experiment condition approach to actual situation. HPLC was applied to study the oxidation kinetic of abietic acid. In addition, intermediate and product of oxidation were tracked and detected by LC-MS. The results provide theoretic support to rosin and its products, wish to solve the problem of easily oxidized

during the storage and manufacture process, which lead to the color fastness and economic losses.

Experimental section

Reagents and instruments

Rosin, produced in Guangxi, China. abietic acid, self-synthesized[4] (98.1%). dehydrade ethanol, diamylamine, hydrochloric acid, acetic acid (AR Grade). GC-MS, Shimadzu GC-MS/QP5050A. HPLC, waters 2487UV/VIS. LC-MS, DionexUltiMate 3000/Thermo Scientific TSQ Quantum Access MAX.

Design of polyethylene film reactor

Polyethylene film was fixed between two aluminum sheets, conducting the micro oxidation reaction of abietic acid. The reactor is shown in scheme 1.

Oxidation of abietic acid

0.1 g of abietic acid was dissolved in 10 mL dehydrate ethanol. 10 μL of as prepared solution was added to PE micro reactor drop by drop[13], in which the film area was $3.0\times1.7 cm^2$. After ethanol was fully vaporized in vacuum under room temperature, reactor was placed in an incubator to perform oxidation, and the kinetic runs were performed between 303 and 333 K. Each sample was taken approximately every 30 min and HPLC was applied to quantitative analysis of both abietic acid and its oxidation products by external standard method.

HPLC conditions

Mobile phase: methanol. flow rate: 1 mL/min. column temperature: 40 °C. wavelength of UV detector: 241 nm/220 nm. chromatograph column: Hypersil ODS2-C18, 5 μm, 250 nm × 4.6 mm. injection amount: 10 μL. external standard method was applied.

LC-MS conditions

HPLC analysis was performed using the Dionex UltiMate 3000 with a binary pump, an on-line degasser, an auto-sampler and a column temperature controller. Chromatographic separation were performed on a Hypersil Gold C18 Column (10 mm × 2.1 mm, 5μm) at 40 °C. The mobile phase consisted of methanol-water (95:5, v/v). The flow rate was set at 0.2 ml/min. Aliquots of 2 μL were injected into HPLC system for analysis.

MS analysis was carried out on a Thermo Scientific TSQ Quantum Access MAX triple stage quadrupole mass spectrometer with an electrospray ionization (ESI) source running in a negative-ionization mode. The typical ion source parameters were: Spray voltage: 3500V. Sheath gas pressure (N_2): 5 units. Ion transfer tube temperature: 350 °C. Collision gas (Ar): 1.5 mTorr. Q1/Q3 Peak resolution: 0.7 Da. Scan width: 0.002 Da. The scan dwell time was set at 0.1s for every channel. All data collected in centroid mode were acquired and processed using Xcalibur 2.2 software (Thermo Fisher Scientific Inc., USA)

Kinetics model Ⅰ(consecutive reaction)

The chemical reaction rate (r) is known to be a function of temperature (T) and reactant concentration (c), and the differential equation is,

$$r_a = -\frac{dc_a}{dt} = kc_a^n \quad (1)$$

Where n is the reaction order.

As the references[4-6, 15] reflected: Abietic acid (A) formed peroxide (O) the first, followed by cracking which formed hydroxyl contained oxidized abietic acid (P). Thus, the reaction can be simplified to a consecutive reaction[16].

$$A + O_2 \xrightarrow{k_1} O \xrightarrow{k_2} P$$

Thus, the first step and second step of abietic acid oxidation can be kinetically expressed as formula (2) and formula (3) respectively.

$$r_1 = k_1 c_A \tag{2}$$

$$r_2 = -r_P = -k_2 c_P \tag{3}$$

Where c_A and c_P represent the concentration of abietic acid and oxidation product of abietic acid in the reaction system respectively. k_1 and k_2 represent the rate constant of first step and second step respectively.

Kinetic equations were calculated by detecting the curve of concentration variation of abietic acid and its oxidation product vs. time, as shown in Fig 2. Under the experimental condition, intermediate of the reaction cannot be quantitative analysis, due to the absorption-free by UV spectrum. Meanwhile, some other oxidant expect peroxide may be produced during the first step of oxidation, therefore, the kinetic cannot be calculated by the variation of abietic acid either. Thus, the kinetic equation of first step was computed by theoretical calculation (formula (6)). More details will be shown below.

Kinetics model Ⅱ (parallel reaction)

Prinz[6] reported several oxidation products of abietic acid and its methyl ester under room storage, indicating that peroxide and oxidant were able to coexist during the oxidation process, as they have different reaction sites. Therefore, a possible mechanism based on parallel reaction model was proposed, as shown below:

$$A + O_2 \rightarrow \begin{cases} \xrightarrow{k_3} O \\ \xrightarrow{k_4} P \end{cases}$$

Thus, the kinetic equations can be presented as follows:

$$r_3 = k_3 c_A = -k_3 c_o \quad (4)$$

$$r_4 = k_4 c_A = -k_4 c_p \quad (5)$$

Where k_3 and k_4 represent the rate constant of peroxide and oxidant respectively.

Similarly, the kinetic of oxidation product is based on the experimental data, whereas the other parallel path regards as k_3 can be fitted by theoretical calculation.

Results and discussion

Wavelength of HPLC detection

Abietic acid has a significant absorption in ultraviolet spectroscopy because of the conjugated group. Thus, UV spectra is a suitable detector for HPLC. Moreover, it is necessary to select an appropriate detection wavenumber to analyze abietic acid along with its oxidant. The result was shown in Figure 1, in which curve (a) is pure abietic acid, curve (b) is abietic acid after 3 hours of oxidation, curve (c) is abietic acid after 1 hour of oxidation and curve (d) is blank PE film. Curve a reveals the maxima absorbance of abietic acid locates at 241 nm. Curve b suggests that oxide of abietic acid has no obvious UV absorbance peak. Considering both abietic acid and its oxide have similar absorbance

at 220 nm, we chose this wavelength to detect abietic oxide. UV specture of oxidation immediate is plotted as curve c. It suggests that in range of 210 – 400 nm, the absorbance is almost 0. On the other hand, 200 -210 nm is overlapped by solvent absorbance. Thus it is difficult to set a wavelength to monitor immediate. In conclusion, we use 241 nm to detect abietic acid and 220 nm to detect oxidation product.

Figure 1. Figure 2.

Here we use 180 min of oxidation at 40 °C as an example. Every 30 min, sample was loaded to HPLC and scanned at 241 nm (the rest of liquid phase conditions are the same to 2.4), as shown in figure 2. For clarity, only three samples scanned at 220 nm by HPLC which oxidation after 0 min, 90 min and 180 min were choose for compare. When the detecting wavelength is set as 241 nm, only abietic acid shows absorbance peak (retention time is 4.2 min). When it is 220 nm, both abietic acid and oxidation product can be detected (retention time is 3.3 min). During oxidation, product is increasing and abieticis decreasing as reactant. Thus 241 nm can tell the total change of abietic acid in the system, as well as apparent kinetic of the reaction. The oxidation product is increased as the decrease of abietic acid. Thus absorbance of 220 nm can be used to study kinetic of formation of product.

Apparent kinetic of oxidation of abietic acid

The logarithm of concentrate ($\ln c_A$) was plotted against time (t), in which the concentrate of abietic acid was calculated from working curves, $y=1.988*10^5x+5.914*10^4$.

The linear response of $\ln c_A$ to time suggests that oxidation of abietic acid is pseudo-first order reaction. The rate constant at different temperature (k_a) were calculated.

The neperian of the rate constant of the reaction at different temperature in which abietic acid oxidizes, $\ln k_a$, has linear relationship with 1/T (T represents temperature), and it is expressed as $\ln k_a = -5954T^{-1} + 13.93$, $R^2 = 0.99$. As calculated apparent active energy, Ea, is 49.51 kJ/mol, according to Arrhenius equation, which has an error range (< 5%) with literature[12].

Kinetic of formation of oxidation product

When reacted at as stated temperatures, we used LC data collected at 220 nm to plot $\ln c_P$-t, according to the working curves of oxidation product $y = 5.097*10^4x + 5.723*10^3$. Since $\ln c_P$ has linear relationship with t, the formation of oxidation product is first order reaction. We achieved k_2/k_4 at different temperatures, and plotted them against T. The relationship between $\ln k_2$ and 1/T is linear which can be described as $\ln k_2 = -5780T^{-1} + 13.32$, $R^2 = 0.99$. As calculated active energy $E_2 = 48.06$ kJ/mol, coefficient $A_2 = \exp(13.32) = 6.09\times10^5 min^{-1}$, rate equation is $r_P = r_2 = r_4 = c_p \times 6.09 \times 10^5 \times \exp(-48.06 \times 10^3/RT)$.

LC-MS analysis of oxidation of abietic acid

In order to explore chemical structure information of major products in abietic acid oxidation system, we analyzed the sample that oxidized at 60 °C for 2 hours by LC-MS[17]. Negative-ionization mode was selected to run Q1 scanning on oxidation product. Range of m/z is set as 310 – 400 m/z. Due to complicated composition of oxidation product of abietic acid, we chose three peaks, which have the largest response in MS spectra, to plot TIC. MS scanning focused on main ion (m/z = 317) (a), fragment ion (m/z = 299). main ion (m/z = 333) (c), fragment ion (m/z = 301). main ion (m/z = 349) (b), fragment ion

(m/z = 331) to track target ion and exclude the effect of impurity, as shown in Figure 3. Inspiring by other people's work[18], m/z = 333 can be considered as major product since it has a much higher intensity then m/z = 317 and m/z = 349. Those small peaks around m/z = 317 can be considered as the result of isomerization.

Negative-ionization mode was selected to conduct on m/z = 317, m/z = 333 and m/z = 349. According to molecular mass, m/z = 317 can be confirmed as abietic acid. Refer to ion cracking mechanism involved and reference[19, 20], a difference of 16 between m/z = 333 and 317 suggests hydroxyl contained abietic acid oxide and a difference of 32 between m/z = 349 and m/z = 317 suggests peroxide of abietic acid[4-6]. Thus we assume that during the oxidation, abietic acid oxide and abietic acid peroxide are both formed at same time. It is possible that peroxide will exist in the system as immediate. Comparing TIC with LC spectra at 220 nm, we confirmed that 3.3 min peak on LC spectra is hydroxyl contained abeitic acid oxide and the peroxide has no apparent absorbance.

As discussed above, oxidation of abietic acid contains two steps, formation of unstable peroxide and oxidation pyrolysis of it which forms hydroxyl contained oxide.

Figure 3.

Theoretical computation of the formation of immediate

Based on kinetic data of formation of abietic acid oxide, kinetic of formation of immediate is able to be calculated. By combining theoretical and experimental data using kinetic model Ⅰ and Ⅱ respectively, we proofed our assumption on the mechanism of oxidation.

According to formula (2) and formula (3), Model Ⅰ can be kinetically represented as:

$$r_A = -r_1 = -k_1 c_A \quad (6)$$

$$r_O = r_1 - r_2 = k_1 c_A - k_2 c_O \quad (7)$$

$$r_P = r_2 = k_2 c_O \quad (8)$$

For continuous oxidation, initial parameters will be: $c_A = c_{A0}$, $c_{O0} = c_{P0} = 0$. Thus at ideal condition, formula (6) - formula (8) can be expressed by integration as follows,

$$c_1 = c_A = c_{A0} e^{-k_1 t} \quad (9)$$

$$c_2 = c_o = \frac{k_1 c_{A0}}{k_2 - k_1}(e^{-k_1 t} - e^{-k_2 t}) \quad (10)$$

$$c_3 = c_P = c_{A0}(1 - \frac{k_2}{k_2 - k_1} e^{-k_1 t} + \frac{k_1}{k_2 - k_1} e^{-k_2 t}) \quad (11)$$

in which, $k_2 = 6.09 \times 10^5 \times \exp(\frac{-48.06 \times 10^3}{RT})$. c_O represents the concentration of peroxide.

Considering the parallel reaction, if the reaction is first order with respect to reactant in every paths, the $k_a = \sum_j k_j$, j = 1, 2 , …… . Where k_a represents the apparent kinetic rate constant. Thus, based on formula (4) and (5), model Ⅱ can be expressed as:

$$c_1 = c_A = c_{A0} e^{-k_a t} \quad (12)$$

$$c_4 = c_o = c_{A0}(\frac{k_3}{k_a})(1 - e^{-k_a t}) \quad (13)$$

$$c_5 = c_p = c_{A0}(\frac{k_4}{k_a})(1 - e^{-k_a t}) = c_{A0}(\frac{k_a - k_3}{k_a})(1 - e^{-k_a t}) \quad (14)$$

in which, $k_4 = k_2 = 6.09 \times 10^5 \times \exp(\frac{-48.06 \times 10^3}{RT})$.

Figure 4 presents the fitted curves at each temperature for the oxidation product based on model Ⅰ and model Ⅱ, respectively. It is obvious that the model Ⅰ fitted the experimental data marginally better the model Ⅱ. The relative residuals with reaction time for all compounds and models tested were presented in figure 5, to consider briefly, only a plot at 318 K for instance. The relative width of error bar based on model Ⅱ is more wide then that of model Ⅰ, indicating that the error of model Ⅰ is small. The goodness-of-fit parameters for both models were summarized in table 1, showing that the Akaike information criterion (AIC) of this two models are close in 303 and 313 K, whereas the AIC of model Ⅰ are much smaller than model Ⅱ in a relatively high temperature (upon 318 K). It can be inferred from this data that model Ⅰ fitted the reaction better than model Ⅱ, suggesting that the oxidation process of abietic acid is tend to be a consecutive reaction. The F value of model Ⅰ is much higher than that of model Ⅱ, indicating the model Ⅰ is the best fit for the number of kinetic constants used in the model. More precisely, the coefficient of determination, R^2, for the rate constant of peroxide based on model Ⅰ (k_1) and model Ⅱ (k_3) ranged from 0.966-0.991 and 0.496-0.955, as shown in table 1, indicating that model Ⅱ (the parallel reaction) was inappropriate in the oxidation process of abietic acid, especially under a relative high temperature.

Figure 4. Figure 5. Table 1.

For clarity, fitted curves of abietic acid, peroxide and oxidant vs. time based on kinetic model Ⅰ and model Ⅱ at 303, 318 and 333K was shown in figure 6. It is obvious that, under the temperature of 333 K for model Ⅰ, as shown in figure 6(E), more amount of

oxidant was produced comparing with the theoretical model data. That is due to the side reaction, e.g., the hydroxyl substitution reaction on C7 and C13 caused by the temperature raising[6], which lead to the unsuitable results by using the kinetic model of two steps continuous reaction. Also, rate constant of the formation of peroxide is available by fitting calculation, as listed in table 2, along with k_a and k_2. Further fitting shows active energy of reaction, E_1, is 58.96 kJ/mol. The coefficient, A_1, is $\exp(5.86)=3.51\times10^3 min^{-1}$. Thus rate equation of the formation of peroxide is: $r_1=c_A\times3.51\times10^3\times\exp(-58.96\times10^3/RT)$.

Since $k_2>>k_1$, peroxide formed in the reaction is transformed to epoxide immediately[21]. Thus the first step, which forms peroxide, determines the total reaction rate. Comparing active energies of two reactions[22], we found that $E_1 > E_2$, $A_1< A_2$ and $k_2$is always larger than k_1, which matches experimental result. As a conclusion, total reaction rate is determined by the first step, which is the formation of peroxide, regardless of temperature.

Figure 6. Table 2.

Conclusion

We performed trace amount of oxidation of abietic acid in PE membrane reactor and provided LC analysis method. LC-MS was used to detect immediate and oxide. Based on what we get, we propose following conclusions:

(1) Thermal oxidation process of abietic acid was investigated by comparing the goodness of fitting of the two kinetic models in chemical reaction, and the results reveal a consecutive reaction. In the first step, peroxide is formed, followed by further oxidation which forms hydroxyl contained abietic acid oxide.

(2) kinetic equation of the first step is $r_1=c_A\times3.51\times10^3\times\exp(-58.96\times10^3/RT)$, active energy is 58.96 kJ/mol. the kinetic equation of the second step is $r_2=c_O\times6.09\times10^5\times\exp(-48.06\times10^3/RT)$, active energy is 48.06 kJ/mol. the kinetic equation of the total reaction is $r_a=c_a\times1.12\times10^6\times\exp(49.51\times10^3/RT)$, apparent active energy is 49.51 kJ/mol.

(3) Ea has an error range (< 5%) with literature and the experimental data has a good fitting with model data in the second step. It indicate the reliability of kinetic equation in this paper.

Acknowledgements

We are grateful to the National Natural Science Foundation of China (11462001) , the Yulin City—Guangxi University Scientific and Technological Cooperation Projects (201210505) and the Young People Fund of Guangxi Science and Technology Department (2012GXNFBA053020) for financial support.

ABBREVIATIONS

n reaction order

r_a apparent chemical reaction rate

c_a concentration of total abietic acid

T temperature

t time

313 k_a apparent chemical reaction rate constant

314 E_a apparent active energy

315 E_1 active energy of first step

316 E_2 active energy of second step

317 r_1 chemical reaction rate (first step of consecutive reaction)

318 r_2 chemical reaction rate (second step of consecutive reaction)

319 r_3 chemical reaction rate (the step of producing peroxide in parallel reaction)

320 r_4 chemical reaction rate (the step of producing oxide in parallel reaction)

321 k_1 chemical reaction rate constant (first step of consecutive reaction)

322 k_2 chemical reaction rate constant (second step of consecutive reaction)

323 k_3 chemical reaction rate constant (the step of producing peroxide in parallel reaction)

324 k_4 chemical reaction rate constant (the step of producing oxide in parallel reaction)

325 c_A concentration of abietic acid

326 c_O concentration of peroxide

327 c_P concentration of oxide

328

329

Notes and references

1. R. Ploeger, E. René de la Rie, C. W. McGlinchey, M. Palmer, C. A. Maines and O. Chiantore, *Polymer Degradation and Stability*, 2014.
2. E. Alvarez-Manzaneda, R. Chahboun, J. Guardia, M. Lachkar, A. Dahdouh, A. Lara and I. Messouri, *Tetrahedron letters*, 2006, 47, 2577-2580.
3. B. Gigante, C. Santos, A. Silva, M. Curto, M. Nascimento, E. Pinto, M. Pedro, F. Cerqueira, M. Pinto and M. Duarte, *Bioorganic & medicinal chemistry*, 2003, 11, 1631-1638.
4. G. C. Harris and T. F. Sanderson, *Journal of the American Chemical Society*, 1948, 70, 334-339.
5. A. Enoki, *Wood Research: Bulletin of the Wood Research Institute Kyoto University*, 1976, 59, 49-57.
6. S. Prinz, U. Müllner, J. Heilmann, K. Winkelmann, O. Sticher, E. Haslinger and A. Hüfner, *Journal of natural products*, 2002, 65, 1530-1534.
7. P. F. Ritchie and L. F. McBurney, *Journal of the American Chemical Society*, 1950, 72, 1197-1200.
8. R. Moore and R. V. Lawrence, *Journal of the American Chemical Society*, 1958, 80, 1438-1440.
9. I. Pastorova, K. Van der Berg, J. Boon and J. Verhoeven, *Journal of analytical and applied pyrolysis*, 1997, 43, 41-57.
10. M. Ladero, M. de Gracia, F. Trujillo and F. Garcia-Ochoa, *Chemical Engineering Journal*, 2012, 197, 387-397.
11. M. Ladero, M. de Gracia, J. J. Tamayo, I. L. d. Ahumada, F. Trujillo and F. Garcia-Ochoa, *Chemical Engineering Journal*, 2011, 169, 319-328.
12. R.-X. QIN, P.-X. HUANG, X.-M. LIU, L. MA and Y.-L. WU, *Chemical Journal of Chinese Universities*, 2009, 5, 024.
13. X.-M. LIU, R.-X. QIN, P.-X. HUANG, J.-L. LIU, L. MA and W.-G. LI, *Acta Physico-Chimica Sinica*, 2010, 26, 2115-2120.
14. J.-L. Liu, X.-M. Liu, W.-G. Li, L. Ma and F. Shen, *Monatshefte für Chemie-Chemical Monthly*, 2014, 145, 209-212.
15. F. Ren, Y.-F. Zheng, X.-M. Liu, X.-Y. Yue, L. Ma, W.-G. Li, F. Lai, J.-L. Liu and W.-L. Guan, *Journal of Molecular Structure*, 2014.
16. M. Möller and H. U. Moritz, *Journal of applied polymer science*, 2006, 101, 4090-4097.
17. J. Cheng, X. Chen, H. Lu, Q. Chen and Y. Zhang, *RSC Advances*, 2014, 4, 43378-43386.
18. E. J. Hsieh, M. S. Bereman, S. Durand, G. A. Valaskovic and M. J. MacCoss, *Journal of the American Society for Mass Spectrometry*, 2013, 24, 148-153.
19. A. Wohlfarth, K. B. Scheidweiler, X. Chen, H.-f. Liu and M. A. Huestis, *Analytical chemistry*, 2013, 85, 3730-3738.
20. R. Liao, H. Wu, H. Deng, Y. Yu, M. Hu, H. Zhai, P. Yang, S. Zhou and W. Yi, *Analytical chemistry*, 2013, 85, 2253-2259.
21. G. Zhu, H. Li, Y. Cao, H. Liu, X. Li, J. Chen and Q. Tang, *Industrial & Engineering Chemistry Research*, 2013, 52, 4450-4454.
22. J. Poudel and S. C. Oh, *Industrial & Engineering Chemistry Research*, 2012, 51, 4509-4514.

374

375

376

377

378

379 **Scheme 1. The polyethylene film reactor**

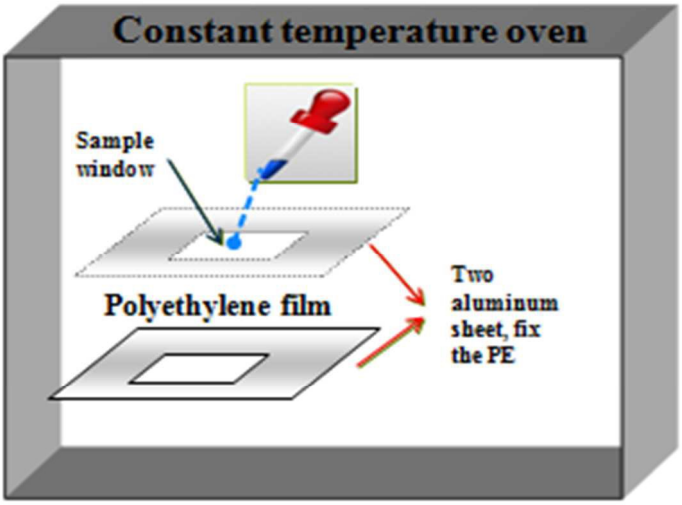

380

381

382

383

384

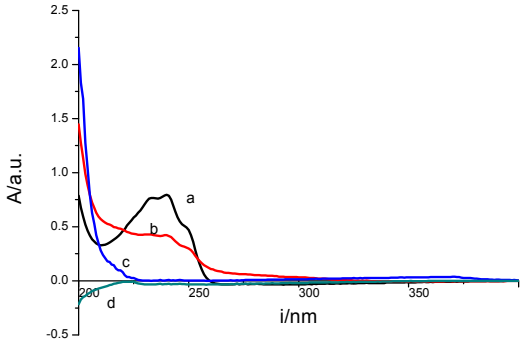

385

386 **Fig.1** UV spectra of the abietic acid oxidation process

387 (a) Abietic acid. (b) Oxide of abietic acid. (c) Intermediate of abietic acid. (d) Blank film

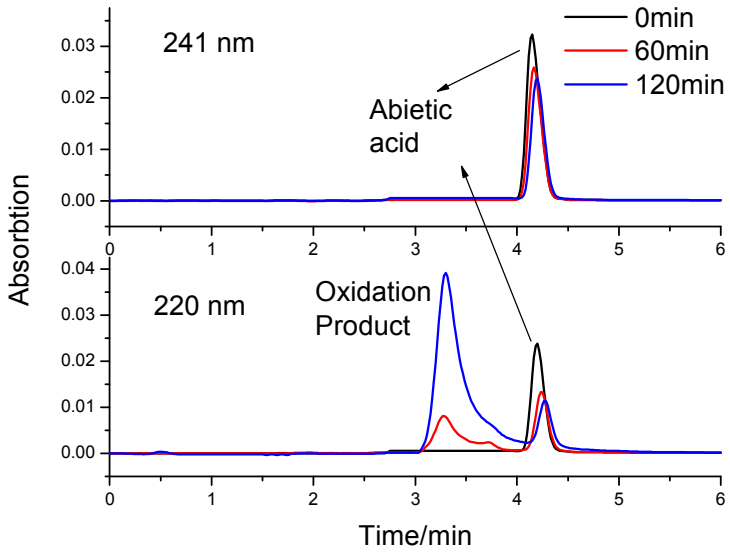

388

389 **Fig.2** HPLC spectra under 241nm/220nm of the abietic acid oxidation process

390

391

392

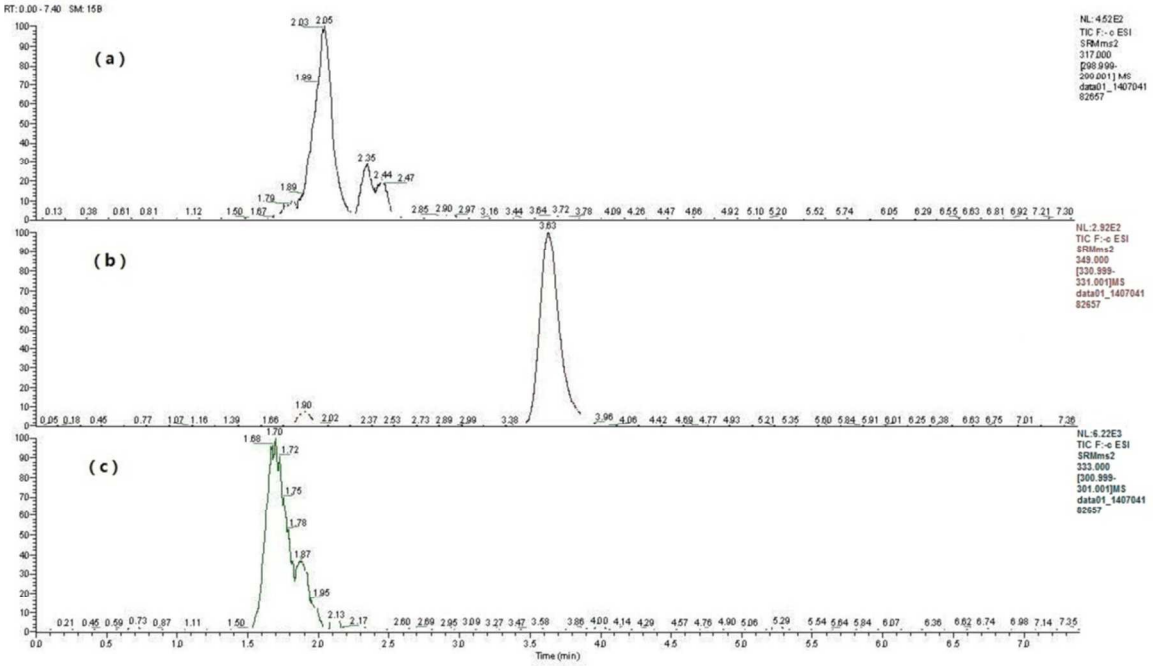

Fig.3 Typical TIC of oxidation system of abietic acid

(a) abietic acid. (b) abietic acid peroxide. (c) abietic acid oxidate

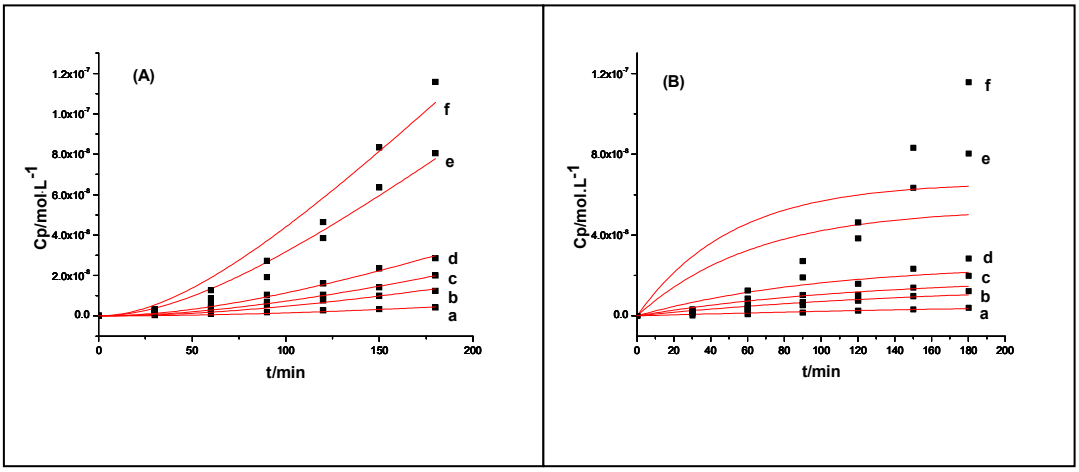

Fig.4 Experimental and predicted results of concentrate of oxidant vs. time profiles based on kinetic model Ⅰ(A) and model Ⅱ (B) at different temperatures. (a) 303K. (b) 313K. (c) 318K. (d) 323K. (e) 328K. (f) 333K.

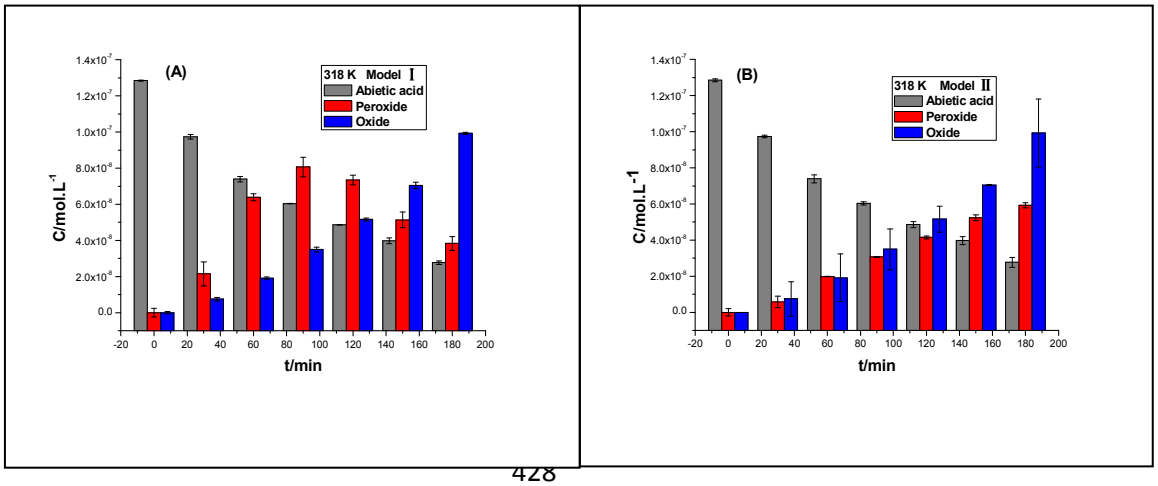

Fig.5 Relative residual concentrations of three compounds (Abietic acid, peroxide, and oxide) that represent the goodness-of-fit of model Ⅰ (A) and model Ⅱ (B) at 318 K.

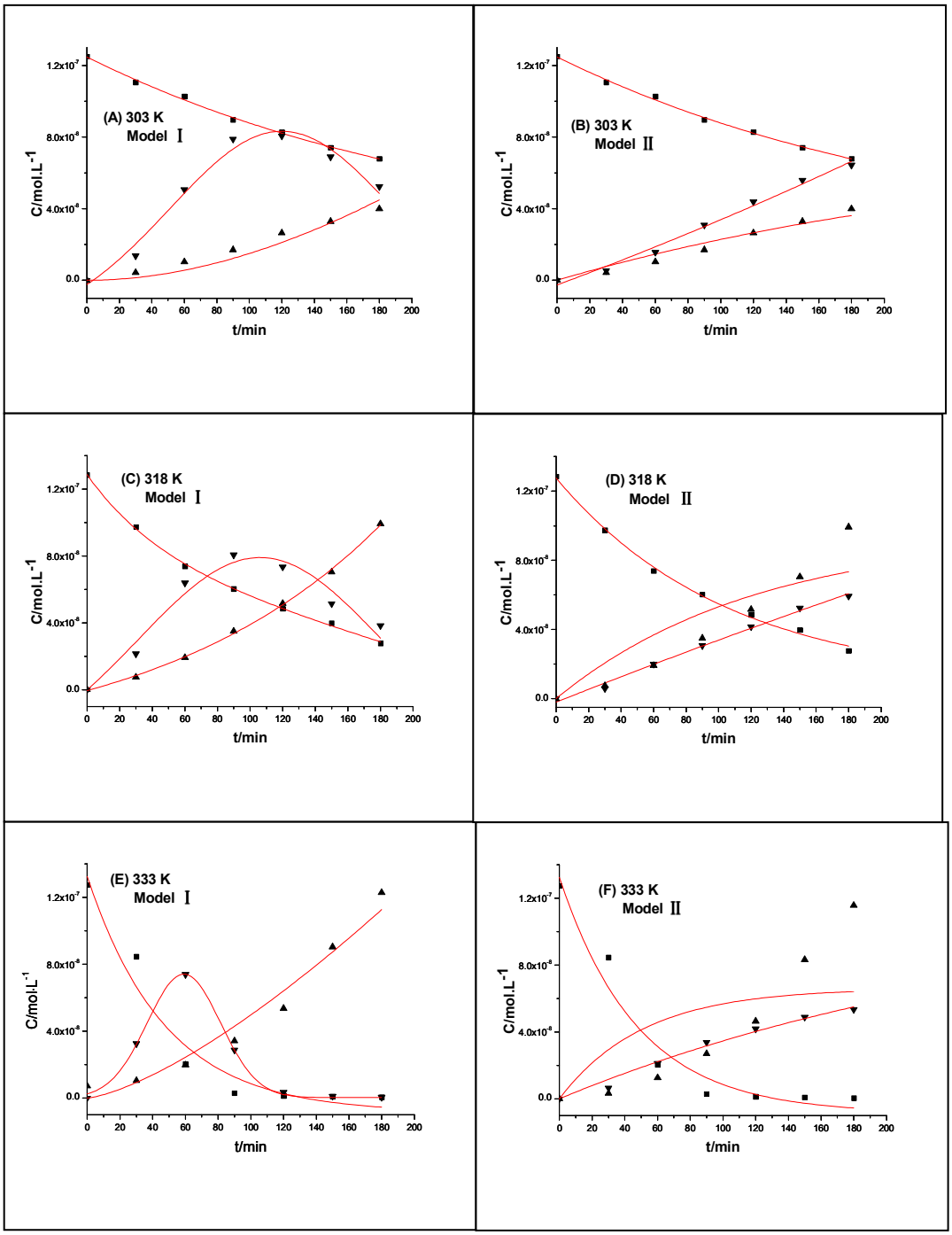

Fig.6 Fitted curves of concentrate of abietic acid■, peroxide ▼ and oxidant ▲ vs. time based on kinetic model Ⅰ and model Ⅱ.

459

460 **Table 1** Goodness-of-fit parameters for model Ⅰ and model Ⅱ.

T/K	Model Ⅰ					Model Ⅱ				
	RSS	RMSE	F	AIC	R	RSS	RMSE	F	AIC	R
303	1.06×10^{-16}	7.59×10^{-18}	207.46	-296.32	0.990	6.00×10^{-19}	4.29×10^{-20}	371.93	-300.32	0.955
313	6.38×10^{-18}	4.56×10^{-19}	320.84	-283.78	0.987	1.01×10^{-17}	7.21×10^{-19}	200.76	-280.57	0.920
318	2.73×10^{-18}	1.95×10^{-19}	1675.68	-289.72	0.991	5.76×10^{-17}	4.11×10^{-18}	73.69	-268.38	0.812
323	6.48×10^{-18}	4.63×10^{-19}	1617.07	-283.67	0.990	1.41×10^{-16}	1.01×10^{-17}	68.32	-262.08	0.801
328	1.19×10^{-16}	8.48×10^{-18}	621.93	-263.31	0.979	2.49×10^{-15}	1.78×10^{-16}	23.96	-242.01	0.580
333	3.96×10^{-16}	2.83×10^{-17}	348.64	-254.88	0.966	5.80×10^{-15}	4.14×10^{-16}	18.17	-236.08	0.496

461 Note: RSS (sum of squared residuals), RMSE (root-mean-square-deviation), F (Fisher F value), AIC (Akaike parameter)

462

463 **Table 2** Kinetic constant of abietic acid at different reaction temperatures

T/K	ka/min^{-1}	$10^{-6}k_1$/min^{-1}	k_2/min^{-1}
303	0.00339	0.0274	0.00305
313	0.00597	0.0481	0.00610
318	0.00811	0.0604	0.00783
323	0.01002	0.0788	0.00988
328	0.01557	0.1682	0.01473
333	0.01958	0.2180	0.01651

464

465